Test of an X-band Doppler polarimetric radar combined with a Doppler LIDAR for wind shear detection at Nice Airport


Clotilde Augros

Clotilde Augros[1], Pierre Tabary[2], Dominique Davrinche[3], Eric Schwartz[4]

[1]*Météo France, DSO/CMR, 42 avenue Coriolis 31057 Toulouse, France, clotilde.augros@meteo.fr*

[2]*Météo France, DSO/CMR, 42 avenue Coriolis 31057 Toulouse, France, pierre.tabary@meteo.fr*

[3]*Météo France, DSO, 42 avenue Coriolis 31057 Toulouse, France, dominique.davrinche@meteo.fr*

[4]*Météo France, DIRSE/CDM06, aéroport de Nice-Côte d'Azur*
06281 Nice, France, eric.schwarz@meteo.fr

(Dated: 10 Mai 2012)

1. Introduction

Abrupt changes in the wind velocity or direction near the ground can cause serious hazards to aircraft during approach or departure operations. That is why the French Air Navigation Service Provider (DSNA) has requested Météo France to design reliable, appropriate and cost-efficient “all-weather” technical solutions to detect, quantify and alert on the presence of low-level wind shear at a number of French airports.

The Nice-Côte d'Azur airport has been chosen as the first evaluation platform of the solutions proposed by Météo France. Its location between sea and mountains and the runway directions parallel to the coast line are main reasons for either clear air or convection wind shears disturbing air traffic. In 2009, a Doppler lidar was installed for 2 months, in order to test its capacity to detect wind-shear. The conclusions indicated that this instrument is well adapted for clear air detection of wind shear (Dabas et al, 2010). In 2011, a second real-time experiment was set up, combining a Doppler 3D lidar and an X-band Doppler polarimetric radar, in addition to 5 anemometers, in order to have an all-weather detection and monitoring of wind shears around the airport (Augros et al, 2011). This approach is in line with several past or ongoing developments elsewhere in the world, such as, the instrumental set-up of the Hong-Kong airport (Chan et al., 2006) or the German project to equip the airports of Munich and Frankfurt with lidar-radar couples.

This experimentation, named « Nice 2011 », started in April 2011 with the installation of a Doppler lidar at Nice airport. The X-band Doppler polarimetric radar was set up in May and the experiment ended in November. The main objective of the experimentation was to evaluate the interest of the radar/lidar system, in association with the ground wind stations, to better anticipate the occurrence of wind shear events on the airport under clear air or rainy events.

For the radar in particular, the technical objectives, were:

- to specify the optimal scanning strategy, in order to combine excellent high-resolution Doppler data quality and good scanning of the volume around the airport and thus better observe and anticipate wind shear events.
- to evaluate whether the ground clutter filter algorithm proposed by SELEX is efficient enough to allow positioning the radar directly at the airport.

This papers first presents the implementation of the instruments at the airport site. The quality of radial velocity is then discussed in relation with the different scanning strategies. The ground clutter spectral filter and the second trip echo filter are next evaluated and an optimal scanning strategy is proposed. To conclude, a wind shear event that occurred at Nice airport during the experimentation is presented, illustrating the interest of the combination of both instruments.

2. Implementation of the X-band radar and the LIDAR at Nice Airport

The LIDAR that has been installed at Nice airport is the WindCube 200S LIDAR from LEOSPHERE. It has a wavelength of 1.54 µm. The maximum range is 6 km for a range resolution of 200 m.
The X-band radar that was rented from SELEX during the experimentation is the METEOR 50DX Doppler polarimetric radar (wavelength of 3.2 cm).
Both instruments were placed at the airport site as illustrated Fig. 1. The 5 minutes scanning strategy of the lidar included 3 RHI at 44°, 224° (runway direction) and 335° (Var valley direction), and a PPI at 3° elevation, which corresponds to the gliding slope of landing airplanes.

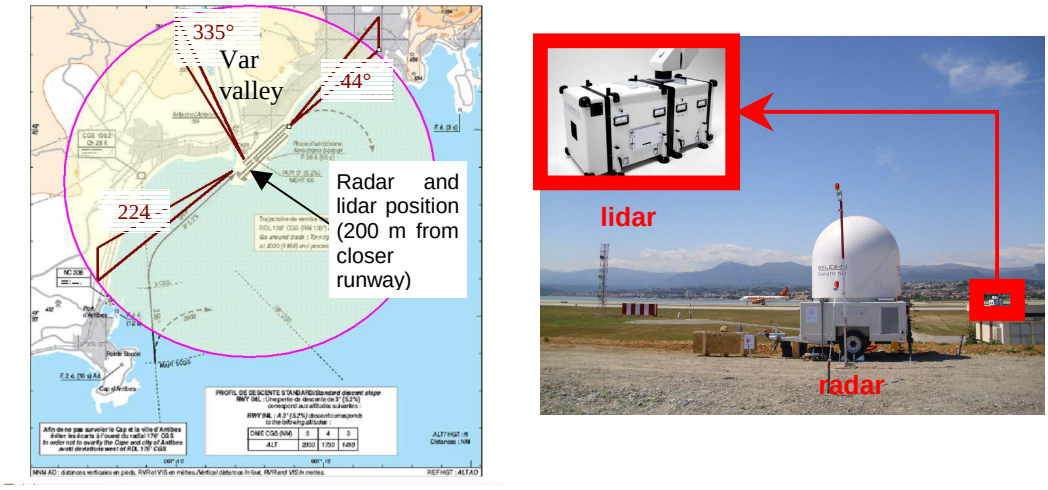

Fig. 1 Runway map at Nice Airport with radar and LIDAR site (left) and picture of radar and LIDAR (right).

Different scanning strategy have been tested for the radar, in order to select the optimal one. They are presented in the two following sections.

3. Evaluation of data quality and specification of an optimal scanning strategy for the radar

3.1. First scanning strategy : evaluation of radial velocity quality

The first scanning strategy of the radar consisted of 11 elevation angles from 1° to 75° in 5 minutes, with the 3° elevation being repeated twice (Fig. 2). Two dual PRF modes were tested : one “low” PRFs mode (1500/1125 Hz) for elevations from 1 to 12°, associated with a rotation rate of 12°/s and one “high” PRFs mode (2000/1600 Hz) for elevations over 12°, with a rotation rate of 36°/s. A lower PRF mode for the lower tilts was chosen in order to reduce the probability of second trip echoes. The radial resolution was set to 150 m in range and 1° in azimuth.

Scan n°	ROT (°/s)	EL(°)	PRF1 (Hz)	PRF2 (Hz)	Vn (m/s)
1	12	1	1500	1125	36,1
2	12	3	1500	1125	36,1
3	12	7	1500	1125	36,1
4	12	12	1500	1125	36,1
5	36	18	2000	1600	64,2
6	36	25	2000	1600	64,2
7	36	35	2000	1600	64,2
8	12	3	1500	1125	36,1
9	36	48	2000	1600	64,2
10	36	60	2000	1600	64,2
11	36	75	2000	1600	64,2

Fig. 2 First scanning strategy

Examples of radial velocity PPIs at elevation 3° and 18° are presented in Fig. 3. The mean quality of radial velocity was evaluated by comparing the raw PPI (with a maximum range of 75 km) against a smoothed PPI obtained by applying a median filter of 7° by 21 range steps (3.5 km), and counting one error if the absolute difference was larger than the smallest Nyquist velocity (Vn2 = 12.1 m/s for elevation 3° and 18 m/s for elevation 18°).
The mean error rate for all radial velocity PPIs of the 05/06/2011 (day associated with convective rain), is 2.36% for elevation 3° and 1.93% for elevation 18°. These error rates are rather low although many error pixels, corresponding to failures of the dealiasing algorithm, are visible on raw velocity PPIs. This is probably because the error pixels, that are mainly at large ranges (more than 30 km) are clearly visible because of their size, which becomes larger with the distance to the radar.

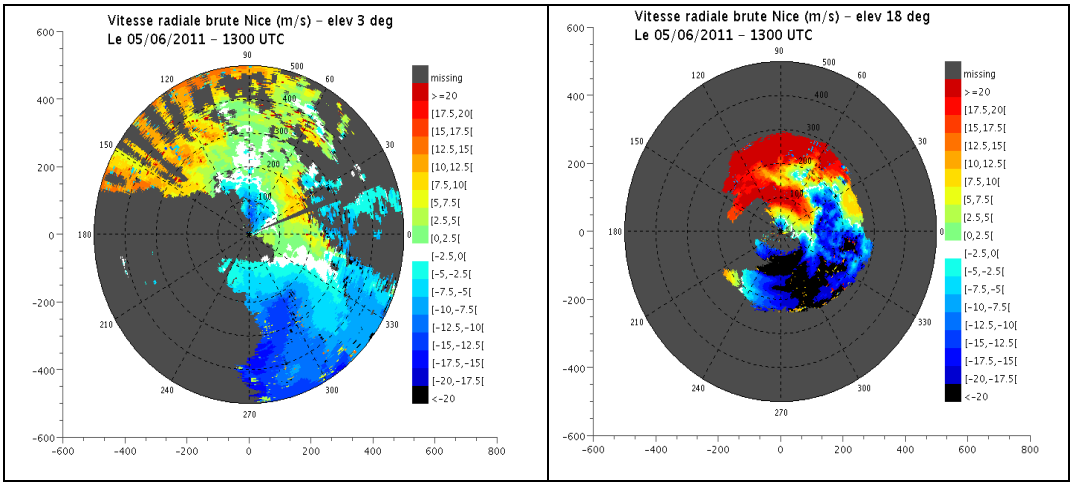

Fig. 3 Radial velocity at elevation 3° (left) and 18° (right). Nice radar, 05/06/2011, 1300 UTC. Maximum range : 75 km.

3.2. Second scanning strategy : selection of the optimal PRF mode for excellent radial velocity quality and evaluation of the Doppler and 2nd trip echoes filters

To further improve radial velocity quality, it was then decided to decrease the antenna rotation speed, and to compare the quality of 3 different PRFs modes using the same elevation angle (3°). The range resolution was increased to 300 m in order to reduce the noise level by integrating over more samples along range. The second scanning strategy is illustrated Fig. 4.
For this scanning strategy, the effects of the Doppler spectral filter and 2nd trip echo filter were also tested, by repeating 3 times each of the 3 PRFs mode : with no filters, with the Doppler filter only and with the Doppler and 2nd trip echo filters.

Scan n°	ROT (°/s)	EL(°)	PRF1 (Hz)	PRF2 (Hz)	Vn (m/s)	Doppler Filter	2nd Trip Filter
1	16	3	1500	1125	36,1	yes	yes
2	16	3	1500	1125	36,1	yes	no
3	16	3	1500	1125	36,1	no	no
4	16	3	2000	1600	64,2	yes	yes
5	16	3	2000	1600	64,2	yes	no
6	16	3	2000	1600	64,2	no	no
7	16	3	2000	1333	32,1	yes	yes
8	16	3	2000	1333	32,1	yes	no
9	16	3	2000	1333	32,1	no	no

Fig. 4 Second scanning strategy

Examples of radial velocity PPI with Doppler and 2nd Trip echo filters for each of the dual PRF modes can be seen Fig. 5. The quality seems close to perfection: no “odd” pixel are visible. The mean quality of each mode was evaluated during the rainy period of this day (from 2000 to 2355 UTC). The dealiasing error rates are : 1.28% for the first mode, 1.47% for the 2nd mode and 0.88% for the 3rd mode.
All these errors rates are very low. As expected, the best mode is the third, because it uses a ratio of PRF significantly less than unity and a high maximum PRF. This PRF mode was therefore selected as the best compromise for the optimal scanning strategy.

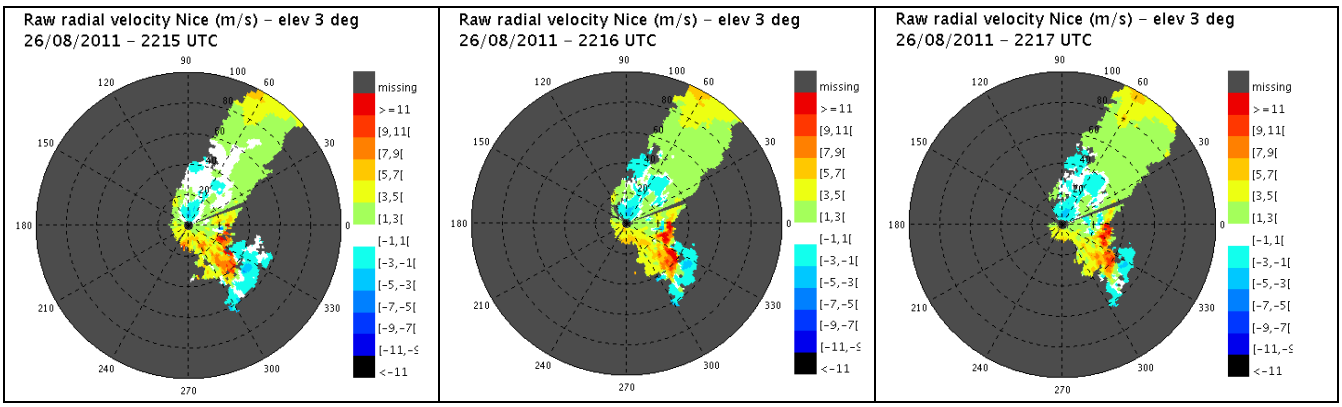

Fig. 5 Radial velocity at elevation 3° for the 3 PRFs modes, from left to right : (1500/1125, 2000/1600, 2000/1333 Hz). Nice radar, 26/08/2011 at 2215 UTC. The PPIs are cut to a maximum range of 30 km (100 range steps).

With the second scanning strategy, it was also possible to test the effect of the Doppler spectral filter and the effect of the second trip echo filter, thanks to the repetition of the same scan with or without activation of these filters (Fig. 4). An example is illustrated Fig. 6. The comparison of the pictures on the right with the middle pictures shows that the clutter filtering is very efficient and enables the retrieval of clear air Doppler echoes that were close to zero before the filtering, because of ground clutter contamination. However, “parasite” echoes persist in the middle images, with positive Doppler values south west of the radar. These echoes are very probably second trip echoes. They are removed in the left pictures but many other valid echoes are also removed.

The analysis of many images revealed that the clutter filter algorithm is satisfying. Yet, the filter tends sometimes to suppress too many weather echoes and could be made less aggressive by adapting the parameters of the ground clutter filter. A sensitivity study should be performed to tune in particular the filter width.
The 2nd trip echoes filter seems essential because strong 2nd trip echoes are frequent with these high PRFs. Nevertheless, this filter reduces clearly the clear air detection threshold. A solution could be to introduce an adaptative signal processing that would deactivate this filter in case there is no rain.

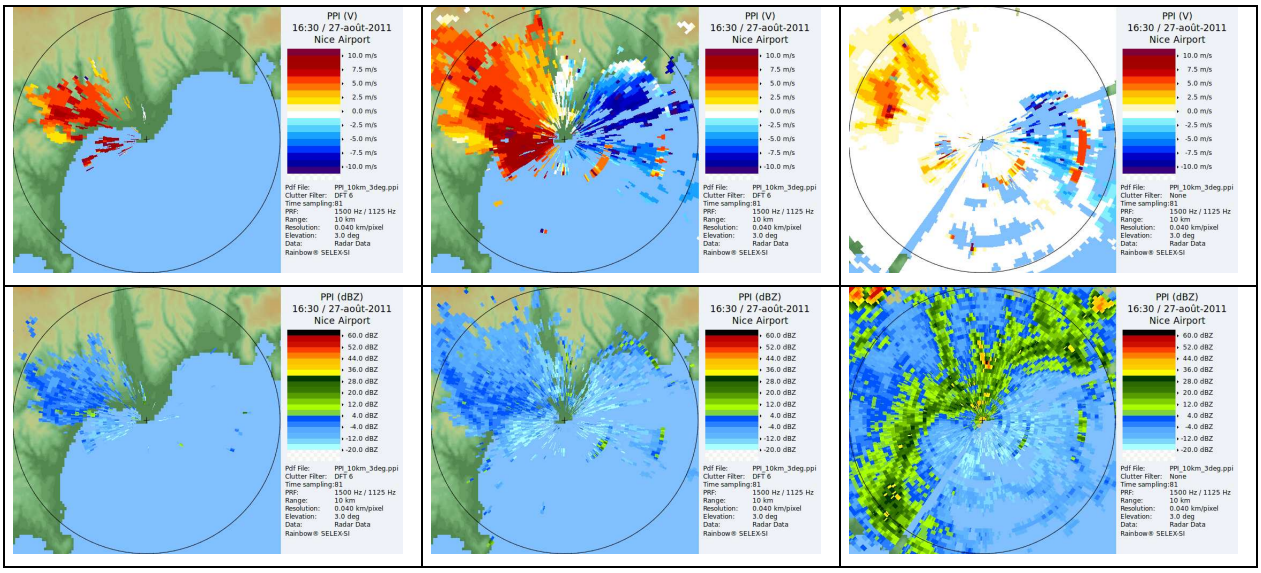

Fig. 6 Radial velocity (top) and reflectivity (bttom) PPIs from left to right : with both filters, with clutter filter only, without any filter. Elevation 3°, PRFs: 1500/1125 Hz. Zoom from 0 to 10 km range.

3.3. Analysis of data at short range

For this experimentation, the radar and the lidar were placed at the airport site although the FAA recommends to place the airport radars at a minimum distance of 8 NMI which corresponds to 14.8 km (Radtec Engineering Inc). It was therefore one of the aim of this experiment to assess if the positioning of the radar at the airport site is satisfying. For that, it was necessary to verify the minimum range that can be seen by the radar. Different situations have been examined. PPIs of reflectivity at 1° elevation, zoomed from 0 to 5 km for a clear air case and a rainy case are illustrated Fig. 7. No minimum range is visible for the PPIs without filtering. A minimum range of about 0.6 km is visible on the reflectivity PPI after Doppler filtering for the clear air case. The minimum range is very small (about 0.1 km) for the rainy case.
The minimum visible range clearly depends on the level of ground clutter close to the airport and the intensity of reflectivity due to rain (or clear air). This is due to the clutter correction ratio (CCOR) of 30 dB set in the clutter filter algorithm. This means that the weather signal (filtered reflectivity) can not be lower than the total reflectivity (ground clutter + weather contribution) minus 30 dB.

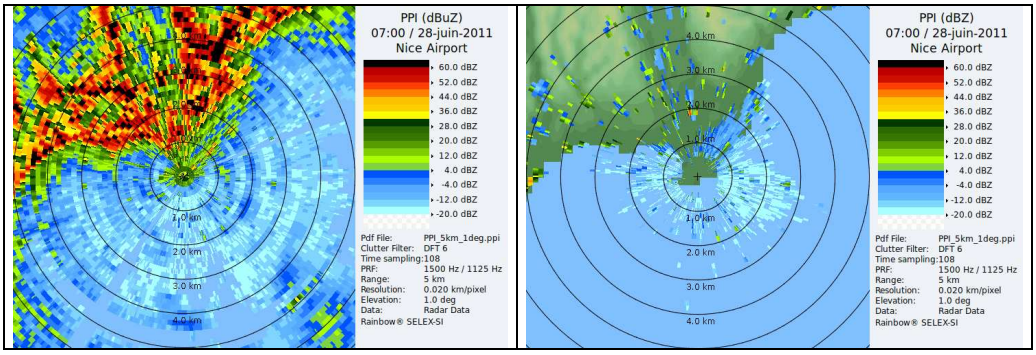

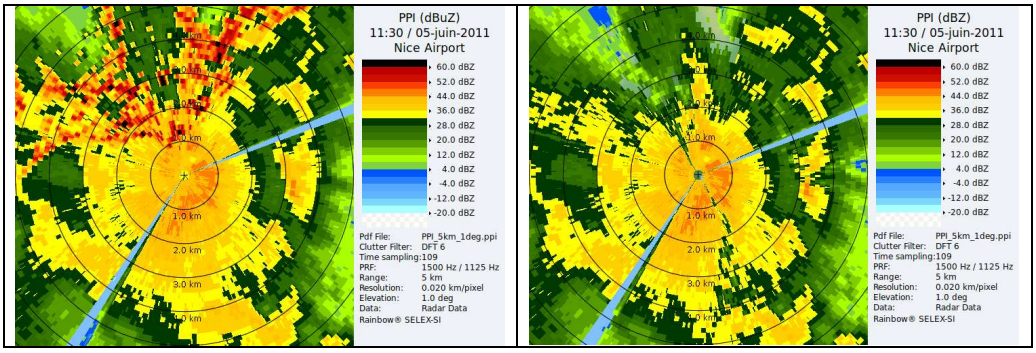

Fig. 7 Reflectivity without filtering (left) and with clutter filtering (right) for a clear air case (28/06/2011 at 0700 UTC) and a rainy case (05/06/2011 at 1130 UTC). Nice radar, elevation 1°. Zoom from 0 to 5 km range.

3.4. Specification of an optimal scanning strategy

After testing of different dual PRF modes, different rotation velocities, a final "optimum" scanning strategy was chosen, starting with an RHI from 1 to 179 ° in the runway direction (like for the lidar), followed by 10 PPIs from 1 to 50° with an optimal dual PRF mode for radial velocity quality of 2000/1333 Hz, with 300 m range resolution and a relatively slow rotation rate of 16°/s. The elevation 3° was repeated twice. To reduce the rotation rate, the higher elevation angles (over 50°) were removed because the forecasters did not consider them useful (they were mainly focusing on low levels). No RHI was proposed in the direction of the Var valley (335°) as done for the lidar but instead, a "pseudo" RHI (VCUT) was built as a real time product by the radar software, using data from all PPIs.

Scan n°	ROT (°/s)	EL(°)	AZ(°)	PRF1 (Hz)	PRF2 (Hz)	Vn (m/s)	ang res (°)	pulse width (µs)	range res (m)	Max range (km)
RHI	6	1-179	44	2000	1333	32,1	0,3	0,5	300	75
1	16	1	/	2000	1333	32,1	1	0,5	300	75
2	16	2	/	2000	1333	32,1	1	0,5	300	75
3	16	3	/	2000	1333	32,1	1	0,5	300	75
4	16	7	/	2000	1333	32,1	1	0,5	300	75
5	16	12	/	2000	1333	32,1	1	0,5	300	75
6	16	18	/	2000	1333	32,1	1	0,5	300	75
7	16	25	/	2000	1333	32,1	1	0,5	300	75
8	16	35	/	2000	1333	32,1	1	0,5	300	75
9	16	3	/	2000	1333	32,1	1	0,5	300	75
10	16	50	/	2000	1333	32,1	1	0,5	300	75

Fig. 8 Final scanning strategy

4. Illustration of the interest of the radar/lidar system for the detection of wind shear during a thunderstorm event at Nice airport

On the 19/10/2011, a convective situation affected the region of Nice in a west to south-westerly flow, from 1600 UTC. The final approach of landing airplanes was from the east, and the different radar and lidar products show a possible turbulence just before the landing because of a northerly wind close to the airport, revealed by the ground stations but also by the radar and lidar RHI toward the Var valley. A few pixels also indicate an easterly wind component around 2 to 3 km from the radar, very close to the ground which can induce a weak wind shear just before the landing. This case was very complex with the orientation of winds changing very fast. The combination of lidar, radar and wind ground stations clearly helps forecasters to better understand the situation. In this case, they could have indicated to the control tower the probable occurrence of turbulence just before the landing.

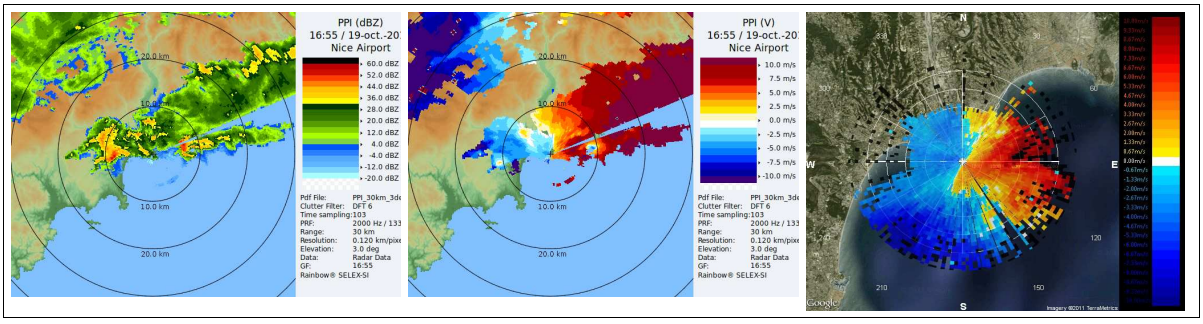

Fig. 9 Radar reflectivity and radial velocity (middle), lidar radial velocity (right). Elevation 3°. 19/10/2011 at 1655 UTC, Nice.

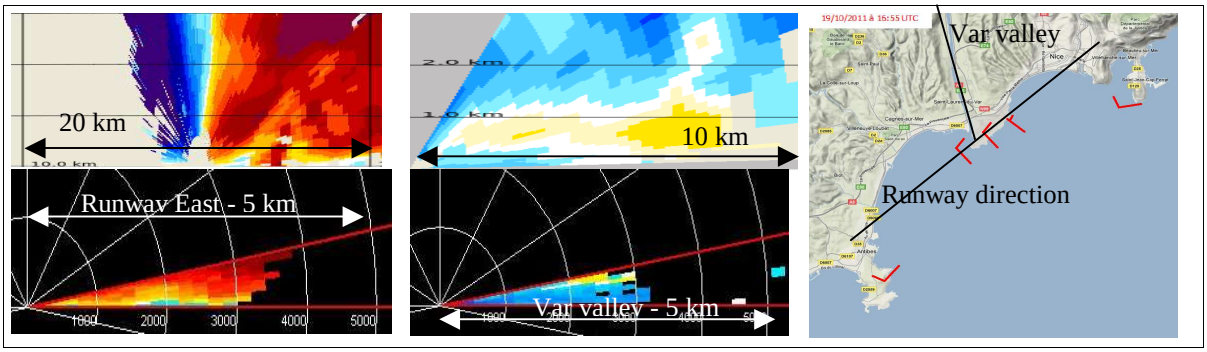

Fig. 10 RHI of radial velocity in the runway direction seen by the radar (top left) and by the lidar (bottom left. Radar pseudo RHI toward the Var Valley (middle top) and Lidar RHI in the same direction (middle bottom). Wind measured by ground station (right) with indication of the directions of the RHIs. 19/10/2011 at 1655 UTC.

5. Conclusion and perspectives

The main objectives of Nice 2011 experimentation was to evaluate a lidar/radar system installed at the airport site for wind-shear detection. Some technical questions have been investigated on the radar side: different scanning strategies were tested and an optimal one was proposed, allowing a very good quality of radial velocity and a good volume exploration. The ground clutter algorithm was satisfying with the default parameters, but improvements could be done in the future by testing different parameters in order to make the filter less aggressive. The second trip echoes filter proved to be necessary and efficient although it removes clear air signal. This could be avoided by deactivating this filter in case there is no rain.

This experimentation showed that the association of lidar and radar at the airport is very useful for wind-shear detection. However, an intense formation for the forecasters is necessary because the wind shear situations are often very complex and it is also not easy for them to react quickly because of the great number of products brought by these instruments. No automatic wind shear warning has been tested during this experimentation and this is another important aspect that should be investigated before operational use.

References

Chan, P. W., C. M. Shun, and K. C. Wu, 2006: Operational LIDAR-based system for automatic windshear alerting at the Hong Kong International Airport. Preprint, 12th Conf. on Aviation, Range, and Aerospace Meteorology, Atlanta, GA, Amer. Meteor. Soc., http://ams.confex.com/ams/pdfpapers/100601.pdf

Dabas et al, 2010 : Lidar Wind-Shear Detection : Nice Airport Trials. Presentation, “Wake vortex and wind monitoring sensors in all weather conditions” workshop, WAKENET-3 Europe / GREENWAKE.

Augros et al, 2011: Test of a combined X-band Doppler polarimetric radar & Doppler lidar system for all-weather wind shear detection at Nice Airport. Poster, 35th Conf. On Radar Meteorology, Williamsburg, Amer. Meteor. Soc., http://ams.confex.com/ams/35Radar/webprogram/Paper191953.html

Radtec Engineering Inc., The Practical Physics Of Airport Weather Radar http://www.radar-sales.com/PDFs/Windshear_3.pdf